

Automatic identification of oil spills on satellite images

Iphigenia Keramitsoglou^{a,*}, Constantinos Cartalis^a, Chris T. Kiranoudis^b

^a*Remote Sensing and Image Processing Team, Department of Applied Physics, University of Athens,
Panepistimioupolis, Build PHYS-V, Athens GR-15784, Greece*

^b*Department of Process Analysis and Systems Design, School of Chemical Engineering, National Technical University,
Zografou Campus, Athens GR-15780, Greece*

Received 22 May 2004; received in revised form 11 November 2004; accepted 27 November 2004

Available online 6 February 2005

Abstract

A fully automated system for the identification of possible oil spills present on Synthetic Aperture Radar (SAR) satellite images based on artificial intelligence fuzzy logic has been developed. Oil spills are recognized by experts as dark patterns of characteristic shape, in particular context. The system analyzes the satellite images and assigns the probability of a dark image shape to be an oil spill. The output consists of several images and tables providing the user with all relevant information for decision-making. The case study area was the Aegean Sea in Greece. The system responded very satisfactorily for all 35 images processed. The complete algorithmic procedure was coded in MS Visual C++ 6.0 in a stand-alone dynamic link library (dll) to be linked with any sort of application under any variant of MS Windows operating system.

© 2004 Elsevier Ltd. All rights reserved.

Keywords: Oil spills; SAR; Remote sensing; Sea surface; Marine pollution; Fuzzy logic

Software availability

Name of software: Oil Spill SAR detector

Developer: Chris T. Kiranoudis, Assistant Professor,
Department of Process Analysis and Systems
Design, School of Chemical Engineering, Na-
tional Technical University, Zografou Campus,
Athens GR-15780, Greece. E-mail: kyr@chemeng.ntua.gr

Hardware required: any PC configuration

Software required: MS Windows

Program language: MS Visual C++ 6.0

Program size: 10 MB

* Corresponding author. Tel.: +30 210 727 6843; fax: +30 210 727 6774.

E-mail address: ikeram@cc.uoa.gr (I. Keramitsoglou).

1. Introduction

Environmental protection is currently an important subject of increasing public concern and as a result, particular attention is being paid to the environmental damage caused by the creation of spills of hydrocarbon compounds over the sea surface created as a result of oil-tanker accidents or illegal cleaning of tankers. A successful combating operation to a marine oil spill depends on the rapid response from the time the oil spill is detected. In fact, the concept of oil spill contingency planning refers to several activities for developing an immediate response program and undeniably the most important one is oil spill detection (Assilzadeh and Mansor, 2001). In fact, several studies have already been reported on oil spill contingency planning (Uthe, 1992; Monk and Cormack, 1992; Theophilopoulos et al.,

1996; Assilzadeh et al., 1999); all studies recognize the oil spill detection and surveillance issue as the most important one amongst all others including assessment and evaluation, spill evolution computer simulation, management and clean up. Oil spills depending on the exact hydrocarbon content and type involve normally extensive areas of film on sea surface, a fact which reduces water roughness and can therefore allow the detection by Synthetic Aperture Radar (SAR) images. It is important that oil spill detection algorithms provide the user with accurate information about specific features characterizing the oil spill, including location of its centroid, size, distance from the land etc. This information has to be available fast and subsequently fed into models which predict the trajectory and fate of a chemical spill (e.g. Skognes and Johansen, 2004; French McCay and Isaji, 2004) and/or statistical oil-spill risk analysis models, such as the “Oil-spill Risk Analysis” (OSRA) model, driven by analyzed sea surface winds and model-generated ocean surface currents (Price et al., 2004).

SAR imagery is a common medium for detecting oil spills. In some cases, especially when a large number of SAR scenes has to be examined, the image processing and by eye discrimination between oil spills and look-alikes may be a time consuming as well as labor-intensive task (Gade and Alpers, 1999). Several important efforts have already been reported so as to develop an automated detection system that would recognize an oil spill through a SAR image without the intervention of the expert. Such systems retrieve SAR images, referring to the sea regions under consideration, from a corresponding satellite platform and produce alarm notifications when an object on the image is identified as an oil slick. From previous experience, the automatic detection of oil slicks in SAR images is reported as a very complicated task because objects resembling oil spills (often called look-alikes) occur frequently in SAR images, especially in low wind conditions. Most frequently, look-alikes are produced by organic film, grease, wind front areas, land, plankton formations, rain cell, current shear zones and upwelling zones (Hovland et al., 1994). There are cases, where even the most experienced operator cannot discern between a possible oil spill and a look-alike. Actually, an experienced operator is trained to discriminate between oil spills and look-alikes based on experience and prior information on weather conditions, difference in shape, contrast to surrounding and background objects and proximity to land. Thus, a fully automated system should actually resemble the expert’s decisions based on similar criteria, knowledge and rules.

The development of automated or semi-automated systems for oil spill detection is a subject of several efforts reported in literature. Kubat et al. (1998) developed a neural network for the classification of

dark regions detected in a series of nine SAR images that served as a training set of the system. The complexity of such a system as well as the appropriate actions that have to be taken into consideration by potential tool developers in such fields were analyzed in detail. Input to the classifier was straightforward, though image preprocessing was not automated. The classifier had an open architecture of rules so that it could embed user experience in several other fields apart from oil detection. Del Frate et al. (2000) also used neural network architecture for semi-automatic detection of oil spills on SAR images using a set of features characterizing a candidate oil spill as input vector. Solberg and Solberg (1996) and Solberg et al. (1999) produced a semi-automated classifier for oil spill detection, in which the objects with a high probability of being an oil spill were automatically detected. Three different categories of probability (low, medium and high) were recognized. A rational processing procedure was adopted for 84 SAR images utilized. It involved pixel local thresholding based on wind level information, clustering of small pixel objects or partitioning of large pixel objects based on sizing criteria and feeding each individual cluster to a classifier operating on a stochastic processing basis. Ten different object characteristics were identified and classification was based on a Bayesian inference procedure. Fiscella et al. (2000) developed a stochastic classifier based on Mahalanobis statistical tests and classical compound probabilities. A preprocessing tool was used in order to extract pixel objects from SAR images and classified them according to statistical criteria implemented on a total of 14 different characteristics of extracted clusters. Marghany (2004) utilized RADARSAT data for oil slick detection and oil slick trajectory model in the coastal water of Malacca Straits. His approach involved two sub-models: one is containing entropy and homogeneity texture algorithms for oil slick detection, and the second one is containing the oil slick trajectory forecasting model.

In the present work a fully automated system for the identification of possible oil spills that resembles the expert’s choice and decisions has been developed. The system comprises modules of supplementary operation and uses their contribution to the analysis and assignment of the probability of a dark image shape to be an oil spill. SAR images are read, located, land masked, filtered and thresholded so that the appropriate dark areas are extracted. Candidate oil spill objects are fuzzy classified to determine the likeness of each individual object to be an oil spill. The output images and tables provide the user with all relevant information for supporting decision-making. The case study area was the Aegean Sea. The system responded very satisfactorily for all 35 images processed.

2. Image preprocessing

Automatic oil spill detection for SAR images was implemented through a series of computational procedures involving retrieval and storage of SAR image content, locating, land masking, smoothing (filtering), thresholding, segmentation and classification. In almost each step a visual or tabular output is available to the user. The sequence of procedures and the available output in each step are presented in Fig. 1. The complete algorithmic procedure was coded in MS Visual C++ 6.0 in a stand-alone dynamic link library (dll) to be linked with any sort of application under any variant of MS Windows operating system. For presentation reasons a multiple document/view application was developed to serve as a visualization tool for the system's user. The tool also involved an automated ftp downloading utility and the automated oil spill detection alarm system developed.

Low-resolution ERS-1 and -2 SAR images (pixel size at range and azimuth equal to 100 m and 79.5 m, respectively) are used for this study. The identification of patterns and shapes in SAR images require the evaluation of radar signal amplitude from complex pixel value as well as the corresponding geometrical corrections necessary for the image integrity. Low-resolution SAR images are derived from preprocessed 5/5 bit complex raw pixel images appropriately re-sampled for a pre-specified size of a non-overlapping moving window across the image. Such images are geometrically corrected and signal amplitude is introduced as a 16-bit integer number. The format of low-resolution SAR

images comprises a leading header and a series of bytes representing pixel values in rows as scanned by radar beam. Header information is important to correctly import the file and appropriately locate it with respect to a pre-specified coordinate system, since several vital image components are included, such as the longitude–latitude pairs of the four corners bounding image quadrilateral as well as of its centroid, the exact image dimensions in pixels, the exact time that was taken and several more specific information.

Information from leading file header is used to derive the exact coordinates of the image-bounding quadrilateral and therefore automatically locate the image in a coordinate map. To restore the image in its correct position with respect to the background, some further processing is required depending on the ascending or descending path of the satellite. Several different SAR images can be simultaneously viewed within the graphical user interface of the tool, as presented in Fig. 2. The tool is equipped with numerous graphical facilities for appropriate zooming and manipulation of the images and bitmaps studied. In particular, image pixels have to be transposed in an up-side-down direction and west-tilted for the ascending mode and mirrored and east-tilted for the descending mode.

The image projection on a latitude–longitude geographical coordinate system is a quadrilateral whose corner points are included in the image header. Let us consider an arbitrary pixel $I(i,j)$ located on the i -th column and j -th row of an image of N columns and M rows. In tool graphics procedures as well as in the land-masking algorithm, one has to estimate the exact longitude–latitude coordinate of the given image pixel $I(i,j)$ and vice versa, i.e. given the longitude–latitude geographical coordinates of a point $C(x_C, y_C)$, to check whether it is included in the image and estimate its exact image coordinates. The derivation involved in mapping operations is given by a set of equations relating point projections on quadrilateral faces, based on the fact that these points must have similar distance proportions on face projections as the image point has with respect to its rows and columns.

Land masking is a very important operation due to the fact that land regions that are present in the image involve several dark regions and thus, their existence may trick the classification process. In addition, in our case studies that involve mostly images of the Aegean Sea, the situation is more complicated because the images cover lots of small and medium sized islands usually very close to one another. Automatic land masking is performed by appropriately overlaying a polygonal GIS theme of the entire map of Greece and Turkey on the image. Each polygon of the collection is transformed in a regional MS Windows API application region and each of them is appropriately region-subtracted by the original image region. What remains is the sea mask. A coarse GIS theme

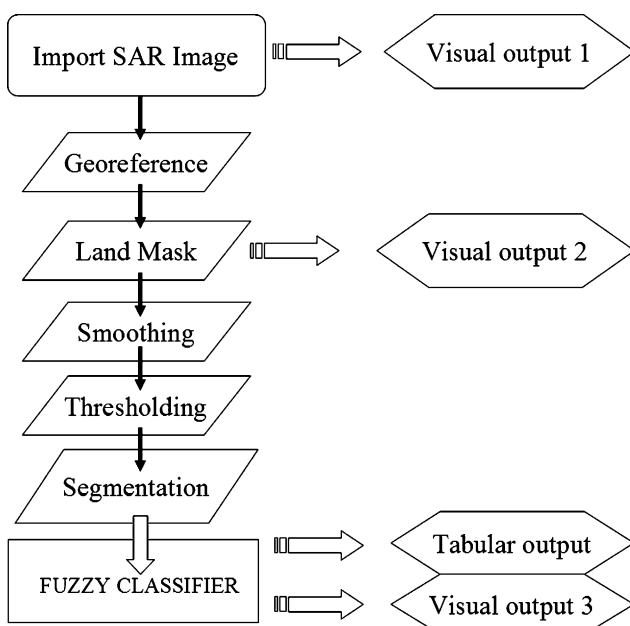


Fig. 1. System information flowsheet.



Fig. 2. Tool main document view.

can be safely used for this purpose for speeding-up calculations. The original polygon regions were created once and used for all images processed.

The sea image pixels are smoothed using a standard Gaussian filter. The Gaussian smoothing operator is a 2-D convolution operator that is used to 'blur' images and remove detail and noise (Davies, 1990; Gonzalez and Woods, 1992). It uses a moving kernel that represents the shape of a Gaussian hump. The moving window size value is 41×41 appropriately tuned. Subsequently, grey-level thresholding was used to segment the image into two classes: one having pixels below a user defined value and one above. This is an important operation for image dark regions extraction. It is applied to each individual image pixel or group of pixels on a local or global level. The pixel digital number is compared to the mean value of all pixels digital numbers lowered by a threshold value. In the case of global thresholding, the window addressed is the entire image. All pixels corresponding to digital number values lower than the threshold value were registered as pixel of a dark region. In this study, local thresholding was adopted, where the window size, the threshold value and degree of overlap between successive moving windows were the procedure parameters. Only pixels belonging to the sea mask were taken into consideration for the numerical process. Thresholding was appropriately optimized by subtracting and adding in each window move, solely the appropriate columns and rows overlapped by previous moves. A moving average scheme was

used for calculating the window mean digital number. As a result, the complexity of this algorithm was $O(NMw)$, where w is the window size. The window size was the same as for smoothing. The value of optimal threshold value used was 40, while a range of 20–100 was tested for performance.

The result of thresholding was the partitioning of the initial sea part of the image into areas characterized as dark and bright. Extraction of pixel groups that would be candidate objects were fed to the system's classifier. This was automatically performed through appropriate segmenting of the initial group objects. Segmentation was performed by determining the k -groups within the extracted dark region objects (Pal and Pal, 1993). This type of groups are characterized by a certain proximity property for the pixels of the group, that is to say, each pixel in the group has at least one pixel neighbor that is close to the former by a distance of k pixels in any direction. This distance metric adopted was actually the norm of the digital space processed (image). In this way, depending on the value of k , smaller groups could be merged to bigger ones. In our system, the greedy approach of 1-groups was adopted (each pixel had at least one neighbor at a distance of one pixel). This procedure takes a few seconds. An $O(NM)$ complexity algorithm was used to separate groups obtained. The algorithm used a multithreaded code where each pixel checked for its neighbors, which in turn checked for theirs in a recursive way.

3. Estimating the probability of an object to be an oil spill

The probability of each object extracted with the techniques mentioned in the previous section to be an oil spill was estimated using an artificial intelligence fuzzy logic modeling system. The system was initially developed by human experts based on their experience and a large database of available information.

3.1. Fuzzy logic as a modeling tool

Fuzzy logic theory has emerged over the last years as a useful tool for modeling processes which are too complex for conventional quantitative techniques or when the available information from the process is qualitative, inexact or uncertain. Although it is almost four decades since Lotfi Zadeh (1965) introduced the fuzzy logic theory, only recently it became a popular technique for developing sophisticated models and systems. The reason for this rapid development of fuzzy systems is simple. Fuzzy logic addresses qualitative information perfectly as it resembles the way humans make inferences and take decisions. It fills an important gap in system design methods, which is between purely mathematical approaches (e.g. system design), and purely logic-based approaches (e.g. expert systems). While other approaches require accurate equations to model real-world behaviors, fuzzy design can accommodate the ambiguities of real-world human language and logic. It provides an intuitive method for describing systems in human terms and automates the conversion of those system specifications into effective models.

Traditional set theory is based on bivalent logic, where an object is either a member of a set or it is not. Contrary to that, fuzzy logic allows a number or object to be a member of more than one sets and most importantly it introduces the notion of partial membership (Klir and Yuan, 1995). Information flow through a fuzzy model requires that the input variables go through three major transformations before exiting the system as output information, which are known as fuzzification, fuzzy inference, and defuzzification. The three steps are depicted in Fig. 3, which shows the

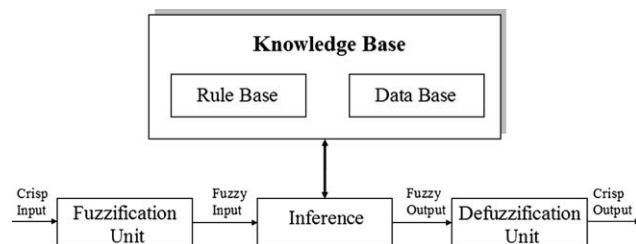


Fig. 3. The structure of a typical fuzzy logic system.

structure of a fuzzy logic system and are explained in brief:

1. *Fuzzification*. It is the process of decomposing a system input variables into one or more fuzzy sets, thus producing a number of fuzzy perceptions of the input.
2. *Fuzzy inference*. After the inputs have been decomposed into fuzzy sets, a set of fuzzy *if-then-else* rules is used to process the inputs and produce a fuzzy output. Each rule consists of a condition and an action where the condition is interpreted from the input fuzzy set and the output is determined from the output fuzzy set.
3. *Defuzzification*. It is the process of weighting and averaging the outputs from all the individual fuzzy rules into one single output decision or signal. The output signal eventually exiting the system is a precise, defuzzified, *crisp* value.

Fuzzy modeling methodologies are procedures for developing the knowledge base of the system, i.e. the set of fuzzy rules (Pedrycz, 1996). The natural way to develop such a system is to use human experts who build the system based on their intuition, knowledge and experience. In this case the fuzzy sets and the membership functions are defined by the experts, usually based on a trial and error approach. The rule structure is then determined based on how the designers interpret the characteristics of the variables of the system.

The most popular fuzzy model suggested in the literature, which is also used in this work, is the one proposed by Mamdani (1974) that has the following formulation with respect to its fuzzy rules:

$$\forall r \in R: \text{ if } \bigwedge_{1 \leq i \leq n} (x_i \in A_i^r) \text{ then } \bigwedge_{1 \leq j \leq m} (y_j \in B_j^r) \quad (1)$$

where r is the fuzzy rule, R is the set of fuzzy rules, \wedge denotes the logical operator “AND”, n is the number of input variables, m is the number of output variables, x_i , $1 \leq i \leq n$ are the input variables, A_i^r , $1 \leq i \leq n$ are fuzzy sets defined on the respective universes of discourse, y_j , $1 \leq j \leq m$ are the output variables and B_j^r , $1 \leq j \leq m$ are fuzzy sets defined for the output variables.

3.2. Development of a fuzzy classifier for the detection of oil spills on SAR images

The fuzzy logic modeling architecture that was used to build a model for the estimation of the probability of an object to be an oil spill was based on important influencing factors. In order to develop the database and the rule base of the system, human experts were employed. The experts used their knowledge and

experience, but also consulted a large database of information, consisting of:

- Database of major oil spill events in the Aegean Sea between 1997 and 1999, provided by the Greek Ministry of Mercantile Marine.
- Information on shape and size of oil spills detected by SAR sensors published in the literature (Solberg et al., 1999; Konings, 1996; Gade and Alpers, 1999).

The Mamdani type of fuzzy model was selected (Mamdani, 1974) and the development of the system was completed in three steps.

1) *Step 1 – Selection of input parameters:* The probability of a dark object on an SAR image to be an oil spill is a function of many factors. The selection of the input parameters was made so that all the important influencing factors are considered, while maintaining the system at a reasonable size. The only source of data was the SAR image itself, making the system completely independent of any external information (e.g. weather and sea condition). Based on the above criteria, the list of selected input variables consisted of the following parameters:

- The total number of objects identified in the image;
- the number of the dark objects in the vicinity of a candidate dark object;
- the area of the candidate dark object;
- the eccentricity of the object's shape;
- the proximity of the object to the land.

It should be mentioned that the wind speed and sea roughness were not selected as input variables explicitly. However, the total number of objects on the image along with the number of dark objects in the vicinity of a candidate dark object are dependent on wind speed and sea roughness, as low wind conditions favor the development of many look-alikes. In moderate wind speed the number of look-alikes is small, and therefore the probability of an object to be an oil spill is higher.

2) *Step 2 – Development of the database:* In this step, fuzzy sets were defined for all the input parameters, as well as for the only output variable, namely, the probability of a dark object to be an oil spill. More specifically, three fuzzy sets were defined for all the input variables, except for the area of the object, for which five fuzzy sets were appointed. An example of the fuzzy set defined for the input variable “total number of objects identified on the image” is given in Fig. 4(a). For the output variable “probability of an object to be an oil spill” the experts defined 3 fuzzy sets which cover the domain from 0 to 1 (corresponding to 0–100%) as shown in Fig. 4(b). A more detailed description of the

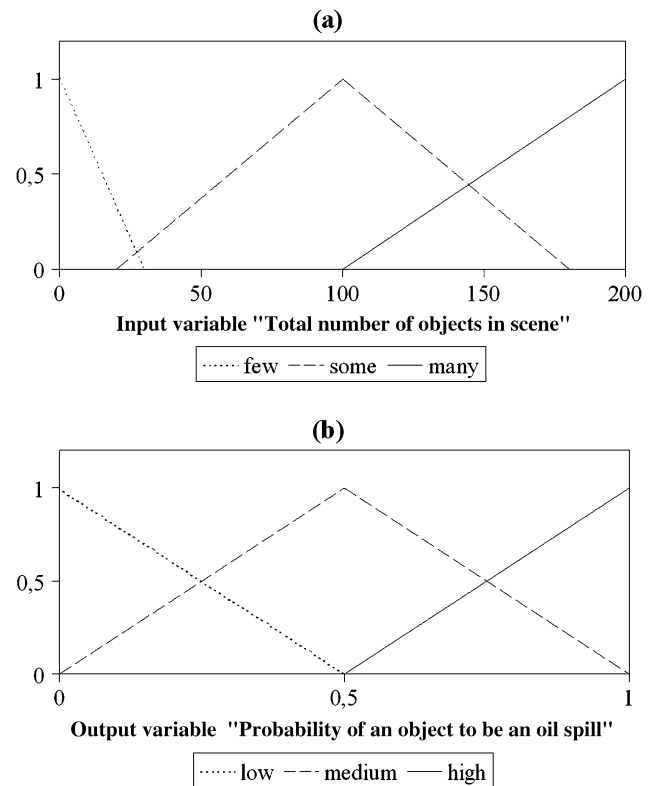


Fig. 4. Fuzzy sets defined for (a) input variable “total number of dark objects in SAR scene” and (b) output variable “probability of a dark object to be an oil spill”.

fuzzy sets appointed to each input or output variable follows:

The total number of objects identified on the image:

Three fuzzy sets, namely “Few”, “Some” and “Many” were defined on the input space which measures the number of objects from 0 to 200 (Fig. 4(a)). The higher the number, the less likely is the observed object to be an oil spill.

The number of the dark objects in the vicinity of a candidate dark object: Again three fuzzy sets, namely “Few”, “Some” and “Many” were defined on the input space. In this case the number varies from 0 to 100, depicting the local conditions. In the case of many dark objects in the vicinity (within 5 km) of the candidate object, it is likely that the observed area is under low wind conditions and therefore the probability of the candidate object to be an oil spill is small.

The area of the candidate dark object in km²: In this case five fuzzy sets were defined, since this parameter is considered crucial for the success of the detection. The range covered by the classes is from 0 to 50 km². Konings (1996) reported that from 283 oil spills observed on SAR images of the North Sea, roughly 62% were less than 1 km², 18% were in the range

1–2 km², 11% were in the range of 2–5 km², 7% were in the range of 5–10 km² and only 2% were larger than 10 km². It has to be noted that these figures were only used as an indication, as the sizes of oil spills in the North Sea are in general larger than the ones observed in the Aegean Sea. However, it can be said with confidence, that the larger the object the smaller the probability to be an oil spill.

The object's eccentricity: The eccentricity of an object is defined as the ratio of the length of the longest chord of the shape to the longest chord perpendicular to it. In more mathematical terms, it is the ratio of the minimum and maximum eigenvalues of shape second order moment matrix. Oil spills are elongated segments characterized by high eccentricities. In the classifier three fuzzy sets were defined, the eccentricity covering the range between 0 and 21.

The proximity of the object to land: Three fuzzy sets were defined, namely “Close”, “Further” and “Away”. The distances cover the range of 0 to 55 km. In general, there are usually many dark objects along the coastline of the leeward side of the islands; therefore, the probability of such a dark object to be an oil spill is low.

Probability of an object to be an oil spill: The only output variable is the probability of an object to be an oil spill and is measured from 0 to 1. For this variable, three triangular fuzzy sets were defined on the above mentioned output space (Fig. 4(b)).

3) *Step 3 – Development of the rule base:* During this step, the experts were employed to develop a number of fuzzy rules, based on their intuition and experience. The fuzzy rules were developed and tuned, so as to relate successfully the input conditions of nine out of the 35

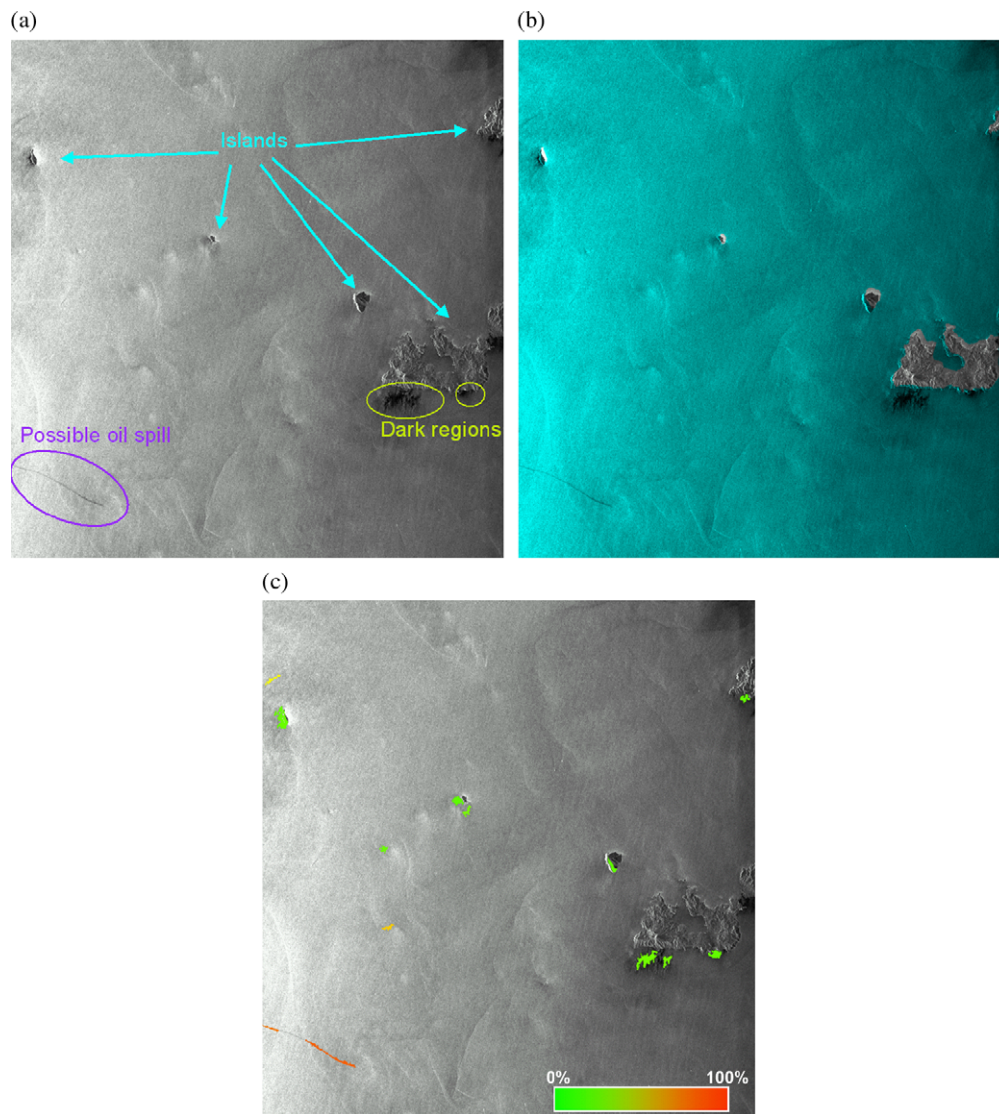


Fig. 5. SAR image with verified oil spill and small total number of dark objects (13): (a) original scene, (b) land masked image, and (c) output image with dark objects colored according to their possibility to be oil spills (green is low, red is high).

available SAR images of the Aegean Sea, acquired under different weather conditions. The images are from the years 1998 and 1999. It has to be stressed that in each image a large number of dark objects are present, potentially oil spills or look-alikes. The number of these objects varies considerably with sea state from around ten to 200 per image. Therefore, the training and subsequent evaluation was based on hundreds of objects.

The rules are constructed in simple language terms and can be understood at a common sense level. At the same time these rules result in specific and repeatable (same inputs gives same output) results. The experts developed 405 rules, one for each combination of fuzzy rules of the input parameters. All the rules use the logical *AND* operation. An example of a fuzzy rule is shown below:


“If the total number of dark objects on image is small *AND* the number of objects in the vicinity of the candidate object is small *AND* the area is small *AND* the eccentricity is high *AND* the distance from land is high *THEN* the probability of the candidate dark object to be an oil spill is HIGH.”

The above three-step procedure defines the knowledge base of the fuzzy system. When the fuzzy model is to be applied to a set of input parameter values, the information flows through the fuzzification–inference–defuzzification processes that are depicted in Fig. 3, in order to generate the fuzzy probability estimation that the candidate dark object is an oil spill. For this particular fuzzy system, the three above processes are executed as follows:

Fuzzification: During the fuzzification process, the triangular membership functions (fuzzy sets) defined on each input variables are applied to their actual values, to determine the degree of truth for each rule premise.

Inference: During the inference process, the truth value for the premise of each rule is computed, and applied to the conclusion part of the rule. This procedure results in the assignment of one output fuzzy set for each rule. The *min–max* inferencing technique was used (Zadeh, 1973), where the output membership function of each rule is clipped off at a height corresponding to the rule premise’s computed

Table 1
Sample tabular output from scene depicted in Fig. 5(a)–(c)

Dark object on image	Number of objects around	Area (km ²)	Eccentricity	Land distance (km)	Longitude (°N)	Latitude (°E)	Probability to be an oil spill (%)
	1	0.843	9.377	32.718	23.58	36.37	76.509
	1	1.081	5.888	5.214	23.41	36.98	50.000
	1	4.587	2.066	0.833	23.45	36.91	21.541
	1	3.124	15.776	44.716	23.72	36.35	80.686
	0	0.994	1.067	16.418	23.73	36.72	21.614
	0	1.002	2.735	23.127	23.78	36.59	59.317
	1	2.019	1.470	1.210	23.87	36.84	19.356
	1	1.097	2.312	1.093	23.90	36.82	24.809
	0	1.383	4.028	0.449	24.24	36.78	19.681
	1	5.048	2.237	2.418	24.35	36.63	23.087
	2	1.590	1.789	2.189	24.40	36.63	23.387
	2	2.210	1.715	0.655	24.50	36.66	20.093
	0	1.542	1.266	1.072	24.45	37.12	19.845

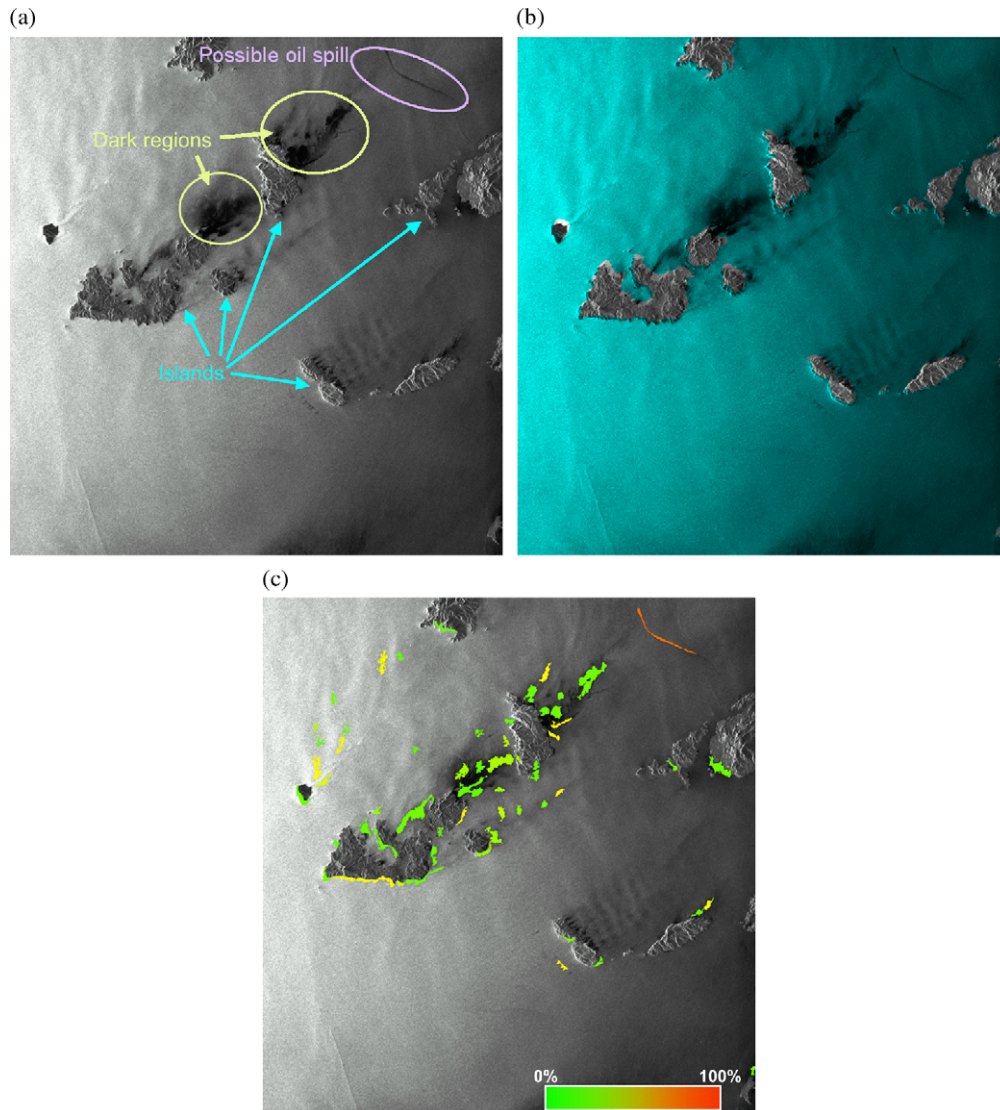


Fig. 6. SAR image with verified oil spill and 59 dark objects adjacent to and between the islands: (a) original scene, (b) land masked image, and (c) output image with dark objects colored according to their possibility to be oil spills (green is low, red is high).

degree of truth. The combined fuzzy output membership function is constructed by combining the results of all the fuzzy rules. If an output fuzzy set is activated by more than one rule, the maximum of all activations is considered in the construction of the combined output membership function.

Defuzzification: The final output of the fuzzy system for the probability of an object to be an oil spill should be a crisp number, so as the fuzzy output needs to be defuzzified. The centroid defuzzification method (Driankov et al., 1993) was used, where the crisp value of the output variable is computed by finding the center of area below the combined membership function.

The programming implementation of the fuzzification, rule-based and defuzzification part of the algorithm was based on numerical analysis approximations

of the problem. More specifically, the area covered within the participation functions as calculated by rules was determined and computed as integral using a Simpson's rule. The fuzzy logic system developed using this approach gives very satisfactory results. The system was applied to the remaining 26 SAR scenes, not included in the training phase, and responded perfectly in 23 of them. The testing also proved that the system can be used to assign a probability that the observed object is an oil spill given any combination of input values within the specified ranges.

4. Case studies

The case study area was the Aegean Sea in Greece. A series of 35 ERS-1 and -2 SAR (acquired in 1998 and

1999) images were tested using the algorithm developed in this study and described above. The algorithms performed satisfactorily in scenes that contained verified oil spills but also in the ones that contained only look-alikes. A set of two images containing verified oil spills is presented (case 1 and 2) together with an example of a complex SAR scene which contained only look-alikes (case 3).

4.1. Case 1





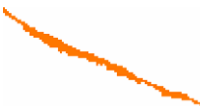





The original SAR image is illustrated in Fig. 5(a) and is the first visual output of the algorithm. The image is acquired over the island of Milos in Cyclades, Greece. The image presents only a small number of dark regions (13 in total) due to moderate wind conditions. The image with the land masked out is illustrated in Fig. 5(b); this is the second visual output in bitmap format. After the thresholding, segmentation and fuzzy classification processes, the result comes out as a third visual output (Fig. 5(c)). In this figure, the candidate objects are painted with colors ranging from green to red, showing the probability of the object to be an oil spill: green is low probability (0%) whilst red is very

high probability (100%). Therefore, when the software is used in an operational mode, the user can immediately depict the areas to be visited for in situ or aerial inspection. The algorithm also generates a tabular output (Table 1) which gives useful information about the scene, such as the number of dark objects around the candidate oil spill, the area of each candidate object (in km²), the eccentricity and proximity to land as well as its geographic coordinates (latitude and longitude in degrees). The table contains the shape of each colored dark object according to its probability to be an oil spill. The algorithm depicted correctly the verified oil spill seen at the SE corner of the image and assigned to it a probability of 80% to be an oil spill.

4.2. Case 2

The original SAR image is illustrated in Fig. 6(a). The image is acquired over the islands of Milos, Sifnos, Serifos and Paros in Cyclades. The image presents a larger number of dark regions compared to Case 1, especially close and between the islands. The total number of dark objects is 59. The image with the land masked out is illustrated in Fig. 6(b); this is the second

Table 2
Sample tabular output from scene depicted in Fig. 6(a)–(c)

Dark object on image	Number of objects around	Area (km ²)	Eccentricity	Land distance (km)	Longitude (°N)	Latitude (°E)	Probability to be an oil spill (%)
	2	0.811	2.750	0.081	24.88	36.63	23.107
	9	10.073	2.760	10.342	24.81	37.09	22.707
	2	1.169	2.650	0.357	24.96	36.60	23.110
	2	1.224	10.723	12.583	24.89	37.22	78.389
	2	2.679	20.210	14.792	24.97	37.19	76.606
	1	1.081	3.579	0.143	25.03	36.97	23.440
	1	1.169	2.596	0.311	25.15	36.72	23.187
	1	1.336	2.738	1.937	25.17	36.74	49.080
	1	5.199	2.915	1.057	25.13	36.98	22.460
	0	0.835	2.548	0.632	25.34	36.47	23.148

visual output of the algorithm. The third visual output is presented in Fig. 6(c). In this case, the algorithm depicted correctly the low probability of the dark objects adjacent to and in between the islands to be oil spills. These formations are due to local low wind conditions. Furthermore, it assigned a high probability of 78% to the verified oil spill shown on the NW part of the image. A sample of the tabular output corresponding to this case study is given in Table 2.

4.3. Case 3

The original SAR image is illustrated in Fig. 7(a). The image presents a very large number of dark regions (117 in total), due to low wind conditions, and no oil spill. Therefore, the dark objects are all look-alikes. The image with the land masked out is illustrated in

Fig. 7(b). After the thresholding, segmentation and fuzzy classification processes, the resultant image is presented in Fig. 7(c). The algorithm depicted correctly that the probability of these objects to be oil spills is low and has left out the very large dark regions, due to their size. The corresponding sample tabular output is given in Table 3.

5. Conclusion

A fully automated system for the identification of possible oil spills has been developed. The software is a stand-alone application for windows. It is only fed by a RAW data satellite image file and returns an alarm as well as all information related to objects detected. The system comprises of modules of supplementary

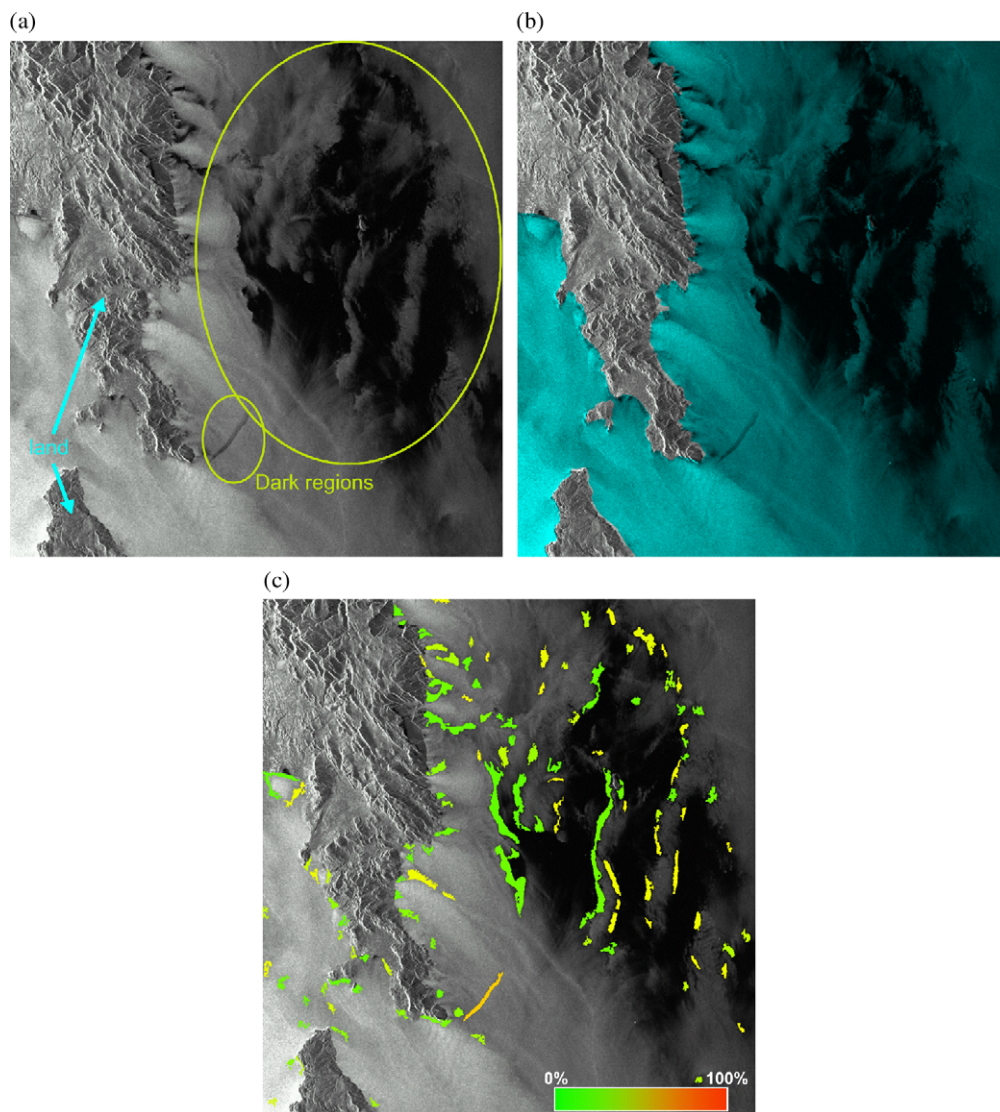
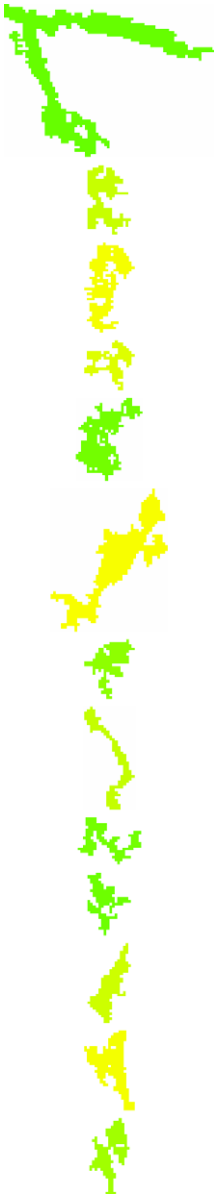


Fig. 7. SAR image containing only look-alikes (117 in total): (a) original scene, (b) land masked image, and (c) output image with dark objects colored according to their possibility to be oil spills (green is low, red is high).

Table 3
Sample tabular output from scene depicted in Fig. 7(a)–(c)

Dark object on image	Number of objects around	Area (km ²)	Eccentricity	Land distance (km)	Longitude (°N)	Latitude (°E)	Probability to be an oil spill (%)
	1	7.131	1.175	1.519	22.72	36.79	20.072
	3	1.614	1.867	9.996	22.76	36.56	39.096
	5	2.202	2.570	12.247	22.79	36.47	48.161
	2	0.938	1.237	3.317	22.86	36.23	43.557
	9	2.465	1.845	9.091	22.83	36.45	22.593
	2	4.333	3.546	1.948	22.77	36.78	48.695
	5	1.200	1.588	1.551	22.88	36.31	27.922
	6	1.081	3.762	0.442	22.91	36.31	38.447
	10	1.129	1.843	2.576	22.89	36.38	22.881
	1	1.010	1.630	4.885	22.89	36.42	21.471
	6	1.296	3.356	0.343	22.83	36.66	40.338
	6	1.781	1.866	2.440	22.85	36.64	48.028
	11	1.375	2.196	1.753	22.92	36.45	31.581

operation and uses the modules for the analysis and assignment of the probability of a dark image shape to be an oil spill. SAR images are read, located, land masked, filtered and thresholded so that the appropriate dark areas are extracted. Candidate oil spill objects are fuzzy classified to determine the likeness of each individual object to be an oil spill. The resulting images and tables provide the user with all relevant information for supporting decision-making. The system was

developed using nine SAR images and was tested independently on 26 images of the Aegean Sea, yielding an overall performance of 88%.

The system can be easily expanded to cover other geographical areas. The time required for the whole process (preprocessing and fuzzy classification) to be completed is of the order of 2–3 min per image, depending on computer speed. In addition, in case of an oil spill alarm, the system provides the operator with

oil spill features necessary as input for trajectory and fate simulation models, such as size, shape, location, and distance from land. Automation of all the above makes the system autonomous; as a result, it can work continuously on a large amount of satellite images and alert the operator in case of an alarm. Therefore, the proposed system can be effectively used in real-time operations.

References

- Assilzadeh, H., Mansor, S.B., 2001. Early warning systems for oil spill using SAR images. In: *Proceedings of the 22nd Asian Conference on Remote Sensing*, Singapore, pp. 358–363.
- Assilzadeh, H., Maged, M., Manson, S.B., Mohamed, M.I., 1999. Application of trajectory model, remote sensing and geographic information systems (GIS) for oil spill emergency response in straits of Malacca. In: *Proceedings of the 20th Asian Conference on Remote Sensing*, Hong Kong, pp. 331–339.
- Davies, E., 1990. *Machine Vision: Theory, Algorithms and Practicalities*. Academic Press, pp. 42–44.
- Del Frate, F., Petrocchi, A., Lichtenegger, J., Calabresi, G., 2000. Neural networks for oil spill detection using ERS-SAR data. *IEEE Transactions on Geoscience and Remote Sensing* 38, 2282–2287.
- Driankov, D., Hellendoorn, H., Reinfrank, M., 1993. *An Introduction to Fuzzy Control*. Springer-Verlag, Berlin.
- Fiscella, B., Giancaspro, A., Nirchio, F., Pavese, P., Trivero, P., 2000. Oil spill detection using marine SAR images. *International Journal of Remote Sensing* 21, 3561–3566.
- French McCay, D.P., Isaji, T., 2004. Evaluation of the consequences of chemical spills using modeling: chemicals used in deepwater oil and gas operations. *Environmental Modelling and Software* 19 (7–8), 629–644.
- Gade, M., Alpers, W., 1999. Using ERS-2 SAR images for routine observation of marine pollution in European coastal waters. *The Science of the Total Environment* 237–238, 441–448.
- Gonzalez, R., Woods, R., 1992. *Digital Image Processing*. Addison-Wesley Publishing Company, 191 pp.
- Hovland, H.A., Johannessen, J.A., Digranes, G., 1994. Slick detection in SAR images. In: *Proceedings of the IEEE Symposium on Geoscience and Remote Sensing (IGARSS)*, Pasadena, CA, pp. 2038–2040.
- Klir, J.G., Yuan, B., 1995. *Fuzzy Sets and Fuzzy Logic: Theory and Applications*. Prentice Hall J, New Jersey.
- Konings, H., 1996. Oil pollution monitoring on the North Sea. *Technical Note. Spill Science and Technology Bulletin* 3, 47–52.
- Kubat, M., Holte, R.C., Matwin, S., 1998. Machine learning for the detection of oil spills in Satellite radar images. *Machine Learning* 30, 195–215.
- Mamdani, E.H., 1974. Application of fuzzy algorithms for simple dynamic plants. *Proceedings of IEE* 121 (12), 1585–1588.
- Marghany, M., 2004. RADARSAT for oil spill trajectory model. *Environmental Modelling and Software* 19 (5), 473–483.
- Monk, D.C., Cormack, D., 1992. The management of acute risks. Oil spill contingency planning and response. In: Cairns, W.J. (Ed.), *North Sea Oil and the Environment: Developing Oil and Gas Resources, Environmental Impacts and Responses*. Applied Science, Elsevier, pp. 619–642.
- Pal, N.R., Pal, S.K., 1993. A review on image segmentation techniques. *Pattern Recognition* 26, 1277–1294.
- Pedrycz, W., 1996. *Fuzzy Control and Fuzzy Systems*. Research Studies Press Ltd, London.
- Price, J.M., Johnson, W.R., Ji, Z.-G., Marshall, C.F., Rainey, G.B., 2004. Sensitivity testing for improved efficiency of a statistical oil-spill risk analysis model. *Environmental Modelling and Software* 19 (7–8), 671–679.
- Skognes, K., Johansen, O., 2004. Statmap—a 3-dimensional model for oil spill risk assessment. *Environmental Modelling and Software* 19 (7–8), 727–737.
- Solberg, A.H., Solberg, R., 1996. A large-scale evaluation of features for automatic detection of oil spills in ERS SAR images. In: *Proceedings of the IEEE Symposium on Geoscience and Remote Sensing (IGARSS)*, Lincoln, NE, pp. 1484–1486.
- Solberg, A.H., Storvik, G., Solberg, R., Volden, E., 1999. Automatic detection of oil spills in ERS SAR images. *IEEE Transactions on Geoscience and Remote Sensing* 37, 1916–1924.
- Theophilopoulos, N.A., Efstathiadis, S.G., Petropoulos, Y., 1996. *ENVISYS, Environmental Monitoring, Warning and Management System*. *Spill Science and Technology Bulletin* 3, 19–24.
- Uthe, E.E., 1992. Application of airborne lidar to oil-spill emergency response decision-support systems. In: *Proceedings of the First Thematic Conference on Remote Sensing for Marine and Coastal Environments*, New Orleans, USA, pp. 159–169.
- Zadeh, L.A., 1965. Fuzzy sets. *Information and Control* 8, 338–353.
- Zadeh, L.A., 1973. Outline of a new approach to the analysis of complex systems and decision processes. *IEEE Transactions on Systems, Man, and Cybernetics* 3, 28–44.